



Habitat Changes of an Endangered Species, the Caucasian Black Grouse, in the Lesser Caucasus Mountains, Iran

ARTICLE INFO

Article Type Original Research

Authors

Sajad Ghanbari, Ph.D.^{1*}
Samira Sasanifar, Ph.D.²
Pedro Álvarez-Álvarez, Ph.D.³
Zeynab Najafi, M.Sc.⁴

How to cite this article

Ghanbari S., Sasanifar S., Álvarez-Álvarez P., Najafi Z. Habitat Changes of an Endangered Species, the Caucasian Black Grouse, in the Lesser Caucasus Mountains, Iran. ECOPERSIA 2025;13(1): 89-105.

DOI:

10.22034/ECOPERSIA.13.1.89

¹ Department of Forestry, Ahar Faculty of Agriculture and Natural Resources, University of Tabriz, Iran.

² Department of Forestry, Faculty of Natural Resources, Urmia University, Urmia, Iran.

³ Department of Organisms and Systems Biology, Polytechnic School of Mieres, University of Oviedo, Asturias, Spain.

⁴ Faculty of Natural Resources, University of Tehran, Karaj, Iran.

* Correspondence

Address: Sajad Ghanbari, Department of Forestry, Ahar Faculty of Agriculture and Natural Resources, University of Tabriz, Iran.
Phone number: 0098-4144237717
P.O.X: 53548-54517
Email: ghanbarisajad@gmail.com

Article History

Received: December 2, 2024

Accepted: February 27, 2025

Published: February 28, 2025

ABSTRACT

Aims: The black grouse (BG) is classified as Near Threatened (NT) by the IUCN due to limited knowledge regarding their optimal habitat conditions. This lack of information has contributed to its inclusion in the endangered species list. The current research examines land-use changes in this species' habitat within the Arasbaran forests of Iran and assesses how conservation efforts have impacted forest cover by quantifying land features.

Materials & Methods: This study analyzed land cover changes in the Arasbaran Region using cloud-free Landsat images from 1987, 2000, 2010, and 2022, obtained from the USGS. The data, preprocessed with Level-1 corrections, were enhanced using vegetation indices like NDVI, GNDVI, MSAVI, and EVI. Atmospheric corrections were applied using the FLAASH model, and areas above 1500 meters were delineated using DEM layers. Four land cover classes—forest, rangeland, agriculture, and bareland—were identified through field surveys and satellite imagery. Land-use maps were created using ENVI's maximum likelihood classification algorithm and validated with accuracy metrics. Temporal changes in metrics from 1987 to 2022 were examined with ANOVA and Tukey's test in SPSS, while PCA identified sensitive variables in CANOCO.

Findings: The findings revealed that over the past 35 years, the forested area designated as black grouse habitat increased by 22%. Consequently, the forest patch area decreased from 5,243 hectares in 1987 to 3,658 hectares in 2022. The most significant change was in forest land, which expanded by approximately 8,907 hectares, mainly due to the conversion of 9,819 hectares from rangeland to forest. From 2000 to 2010, 24.12% of the region experienced changes, the most notable being an increase of 11,667 hectares in agricultural land, primarily from the conversion of 8,195 hectares of rangeland. This has led to a reduction in forest edges and an increase in habitat connectivity. Additionally, there has been a decline in rangeland, agricultural land, and barren land within the BG habitat.

Conclusion: The findings indicate that agricultural lands have transitioned into barren lands over the past 35 years, reflecting the success of protective measures. Furthermore, the results suggest that habitat conditions for the optimal distribution of the BG species in the study area are improving. However, more detailed investigations into population changes of this bird over the past 35 years are needed to fully understand the impact of land-use changes on its population dynamics.

Keywords: Arasbaran Forests; Black Grouse; Landscape Features; Land-Use.

CITATION LINKS

[1] Jantz S.M., Barker B., ... [2] Ghanbari S., ... [3] Xu L., Chen S.S., Xu Y., Li G., Su ... [4] Allan J.R., Watson J.E., Di Marco M., O'Bryan C.J., Poss ... [5] Ndegwa Mundia C., Murayama Y. Analysis of land-use/cover ... [6] Clark N.E., Boakes E.H., McGowan P.J., Mace G.M., Fuller ... [7] Rahdari V., Maleki ... [8] Najafi Z., Darvishsefat ... [9] Foroutan S., Islamzadeh ... [10] Baskaya S. Distribution and principal threats to Caucasi ... [11] Storch I. Conservation ... [12] Darvishi A., ... [13] Kaboodvandpour S., Shiriazar J. Modeling the habitat des ... [14] Darvishi A., ... [15] Etzold J. Analyses of ... [16] Ghanbari S., Nasiri V., ... [17] Ghanbari S., Turvey S.T. Local ecological knowledge prov ... [18] Sagheb-Talebi K., Pourhashemi M., Sajedi T. Forests of I ... [19] Sasanifar S., Alijanpour A., Shafiei A.B., Rad J.E., Mol ... [20] Ghanbari S., Sefidi K., Álvarez-Álvarez P. Vegetation an ... [21] Ghanbari S., Sasanifar S. Agroforestry Systems in Arasba ... [22] Rouse J.W., ... [23] Qi J., Chehbouni A., Huete A.R., Kerr Y.H., Sorooshian S ... [24] Huete A., Liu H., Batchily K., Van Leeuwen W. A comparis ... [25] Muchsin F., Dirghayu D., ... [26] Cooley T., Anderson ... [27] Berk A., Anderson G.P., Bernstein L.S., Acharya P.K., Do ... [28] Yang M., Hu Y., ... [29] Wang Z., Xia J., ... [30] Shalaby A., Tateishi R. Remote sensing and GIS for mappi ... [31] Günlü A., Sivrikaya F., ... [32] Serra P., Pons X., Saurí D. ... [33] Heidarlou H.B., ... [34] Rash A., Mustafa Y., Hamad R. ... [35] Ribeiro M.P., de Mello ... [36] Negassa M.D., Mallie ... [37] Sefidi K., Ghanbari S. ... [38] Faridi E., Naseri D. ... [39] Behruzi Rad B. Biology ... [40] Karami A., Fegghi J. ... [41] Gottschalk T.K., ... [42] Yousefi M., Darvishi ...

Introduction

In recent decades, the reduction of biodiversity has become increasingly apparent, recognized as one of the most significant global changes ^[1,2], drawing wide attention from the international community ^[3]. One of the primary drivers of biodiversity loss is habitat destruction through land-use change ^[1]. Protecting animal and plant biodiversity requires identifying factors affecting these indicators ^[4]. Humans directly impact land-use to meet their needs, altering the landscape pattern. Land-use change is a key factor that affects habitat conditions and significantly influences the distribution of wildlife species. In recent decades, developing countries have experienced unprecedented land-use changes that continually reshape ecosystems and lead to habitat loss and fragmentation ^[5]. Habitat loss threatens the diversity and populations of animal species at both local and global scales ^[6]. Changes in protected wildlife areas significantly impact ecological systems and the distribution of wildlife species. These alterations disrupt the flow of materials and energy between habitat patches, ultimately affecting the capacity and services that these habitats provide ^[3].

To effectively plan and manage human activities that interfere with environmental elements while achieving conservation goals, it is necessary to determine land-use change patterns ^[7]. Satellite information technology provides faster, more accurate, and more cost-effective solutions for continuous land cover monitoring than traditional methods such as aerial photography, ground surveys, or manual mapping. While aerial photography can capture detailed images, it is often more expensive and time-consuming. Ground surveys, though precise, require a significant workforce and can be limited in coverage. In contrast, satellite technology can monitor vast areas quickly

and regularly, allowing for real-time updates and better analysis of land cover changes over time ^[8]. Utilizing land surface indicators as measurable parameters or metrics that reflect the condition and characteristics of the Earth's surface alongside remote sensing techniques enables quantitative evaluation of land surface changes ^[9]. These indicators include vegetation cover, soil moisture, surface temperature, land cover types (e.g., urban, agricultural land, forested areas), and more.

The black grouse (*Lyrurus mlokosiewiczii* Taczanowski) is a valuable species found exclusively in the Arasbaran forests of Iran. It is categorized as endangered in Iran and near-threatened globally ^[10]. The species' distribution range includes the Forest Mountains of Russia, Armenia, Georgia, Azerbaijan, Turkey, and Iran ^[11]. In the Arasbaran Region, BG exists within and outside the Biosphere Reserve. Their habitat comprises a combination of forest and rangeland ecosystems, with nesting occurring under bushes and rocks ^[12]. BG predominantly inhabits northern slopes at altitudes above 1500 meters above sea level ^[13]. Habitat loss or degradation due to human interventions such as land-use change, livestock grazing, rural and nomadic road construction, and hunting poses the most significant threat to their survival ^[14-16].

Several studies have investigated BG populations and factors influencing this species in Iran and other countries. Etzold (2005) described the habitat of BG in Azerbaijan, attributing population decline to human activities such as intense grazing, vegetation burning, and habitat destruction. Excessive grazing was identified as the primary threat to the species in Azerbaijan. Darvishi et al. (2014) examined landscape pattern changes in BG habitat in the Arasbaran Region (1987-2011).

Fragmentation of the landscape disrupted BG habitat in Arasbaran. Kaboodvandpour and Shiriazar (2019) identified topography, land-use, slope, slope direction, and distance from human settlements as essential variables influencing BG habitat desirability in these forests. Ghanbari and Turvey (2022), based on local ecological knowledge in the Arasbaran Region, noted a significant decrease in BG population compared to other wildlife, attributed to habitat destruction from increased livestock grazing ^[17].

The literature review indicates declining BG populations in the Arasbaran Region and globally due to human activities. Detailed studies on its threats are necessary to prevent species extinction. By controlling these factors, the BG's regeneration process can be supported. This study aims to evaluate and quantify landscape changes in BG habitat in the Arasbaran forests and to identify the key indicators influencing these changes. Recognizing the threats to BG habitats underscores the need for effective planning and management strategies to mitigate human impacts and achieve conservation goals. While previous studies have identified human activities such as intense grazing and habitat fragmentation as key threats to BG, this research advances the understanding by employing remote sensing to provide real-time, accurate monitoring of land-use changes over an extended period. It bridges the gap between traditional methods and modern technological approaches, offering a more efficient and scalable solution for continuous habitat evaluation. This is crucial for developing effective conservation strategies in the region. Continuous monitoring of land-use change patterns is crucial for this understanding. The research will utilize satellite information technology for its speed, accuracy, and cost-effectiveness in monitoring land cover changes. The study will quantitatively assess how land-use

changes impact habitat quality and species distribution by integrating remote sensing techniques with land surface indicators. Ultimately, the goal is to inform conservation strategies that can reduce habitat loss and enhance the survival of BG in the region.

Materials & Methods

Study Area

Arasbaran forests are renowned for their unique habitat, which supports high animal and plant diversity, some of which are endangered. Designated as a biosphere reserve by UNESCO in 1976 (18, 19), these forests receive annual rainfall ranging from 300 to 600 mm. The region also serves as a seasonal home for nomadic communities ^[20]. With altitudes ranging from 450 to 2700 meters above sea level, the current research focuses on the habitat of the BG situated at an altitude of 1500 meters above sea level in the Arasbaran Region ^[21] (Figure 1).

Data Collection and Analysis

Cloud-free Landsat 5 TM and Landsat 8 OLI images from September 1987, 2000, 2010, and 2022 (Table 1) were utilized for this study. These images, provided by the United States Geological Survey (<https://earthexplorer.usgs.gov/>) with L1 corrections, including geometric and radiometric adjustments to the raw data, underwent comprehensive preprocessing for further analysis.

Table 1) Specifications of the used Landsat satellite images.

Satellite Name	Sensor	Attainment Date	Number of Bands	Row/Path
Landsat 5	TM	1987-09-21	7	33/168
Landsat 5	TM	2000-09-08	7	33/168
Landsat 5	TM	2010-09-04	7	33/168
Landsat 8	OLI	2022-09-05	9	33/168

Arasbaran Land Cover Dynamics

In the Arasbaran Region, enhancing the accuracy of land cover mapping-an essential

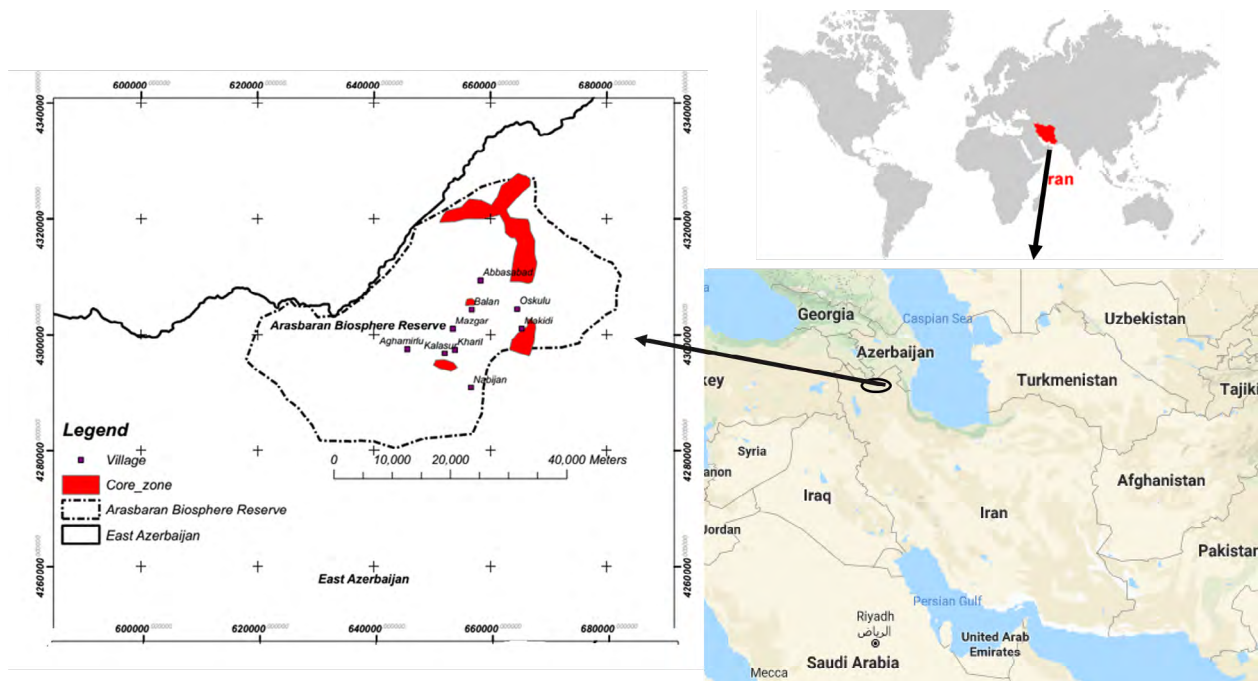


Figure 1) The location of the BG habitat in the Arasbaran Region, East Azerbaijan Province, Iran.

process for environmental monitoring and management—depends mainly on using advanced vegetation indices. These indices, derived from satellite imagery, provide crucial insights into vegetation health and distribution. One of the most widely used indices in this context is the Normalized Difference Vegetation Index (NDVI) [22]. NDVI calculates the difference between near-infrared (NIR) and red light reflected by vegetation, normalized by their sum, effectively highlighting healthy, dense vegetation areas. This makes NDVI a powerful tool for distinguishing between different land cover types, especially in heterogeneous landscapes like Arasbaran, where accurate delineation of forests, grasslands, and other cover types is vital for sustainable land-use planning.

In addition to NDVI, other specialized vegetation indices are utilized to address specific challenges in land cover classification in the Arasbaran Region. For example, the Green Normalized Difference Vegetation Index (GNDVI) replaces the red band with the green band, providing greater

sensitivity to variations in chlorophyll content—essential for assessing plant vigor and stress [23]. The Modified Soil Adjusted Vegetation Index (MSAVI) is designed to minimize the influence of soil reflectance, particularly in sparsely vegetated areas, making it especially reliable in semi-arid environments. Meanwhile, the Enhanced Vegetation Index (EVI) improves upon NDVI by reducing atmospheric interference and soil background noise, offering better performance in densely vegetated regions. By integrating these indices, researchers can significantly enhance the precision of land cover maps in Arasbaran, leading to more informed decisions regarding conservation and resource management [24].

The geometric accuracy of the images was evaluated by overlaying road layers extracted from 1:25,000 topographic maps onto the satellite imagery. Additionally, the radiometric quality was verified by visually inspecting individual bands and various color composites on the screen.

The FLAASH (Fast Line-of-sight Atmospheric Analysis of Spectral Hypercubes)

atmospheric correction method was applied to minimize atmospheric effects. The FLAASH model is a software package developed by the Air Force Research Laboratory, Space Vehicles Directorate (AFRLiVS), Hanscom AFB, and Spectral Sciences, Inc. (SSI) to support the analyses of visible-to-shortwave infrared (Vis - SWIR) hyperspectral and multispectral imaging sensors [25]. FLAASH derives its 'physics-based' mathematics from MODTRAN4 [26, 27]. For the FLAASH parameter setting, any standard MODTRAN model atmosphere and aerosol types can be chosen to represent a scene, and a unique MODTRAN solution is computed for each image [28]. It can correct the cascade effect caused by diffuse reflection and is an excellent atmospheric correction method [29]. The DEM layer isolated areas above 1500 meters altitude for further analysis.

The investigation and field surveys identified four regional land cover classes: forest, rangeland, agriculture, and bareland. Representative samples were introduced into the model to classify these areas. Using the Google Earth database and satellite images from different seasons, a series of points were selected to capture various conditions across the four land cover classes. Efforts were made to ensure an even distribution of training samples. A total of 275 samples were collected, with 192 used for classification and 83 randomly selected for accuracy assessment. A land-use map categorizing forest, rangeland, agriculture, and bareland for areas above 1,500 meters in altitude was generated using the maximum likelihood classification algorithm in ENVI software [30-32].

Accuracy Assessment

Confusion matrices were generated by comparing the validation samples with the land cover maps to assess the accuracy of the Landsat data classification. These matrices are used to calculate general validation metrics such as Overall Accuracy (OA)

and the Kappa Coefficient (KC), as well as individual metrics like User's Accuracy (UA), Producer's Accuracy (PA), and the F-score (FC) [33]. The user's accuracy (Eq. 1) reflects the probability that a pixel has been correctly classified. In contrast, Producer's Accuracy (equation 2) indicates the likelihood that a sample from the image belongs to the correct class. Overall accuracy represents the percentage of correctly classified pixels. It is calculated by dividing the sum of the diagonal elements of the confusion matrix by the total number of pixels (Eq. 3). Due to limitations in Overall Accuracy, the Kappa Coefficient is often used, as it accounts for the misclassified pixels. It compares the accuracy of the classification to what would be expected from a completely random classification. KC values range from 0 to 1 (or 0% to 100%). A Kappa Coefficient above 80% indicates strong agreement, 40% to 80% indicates moderate agreement, and below 40% is considered poor [34].

$$UA = \frac{x_{ii}}{x_{i+}} \quad \text{Eq. (1)}$$

$$PA = \frac{x_{ii}}{x_{+i}} \quad \text{Eq. (2)}$$

$$OA = \frac{\sum_{i=1}^r x_{ii}}{N} \quad \text{Eq. (3)}$$

$$KC = \frac{N \sum_{i=1}^r x_{ii} - \sum_{i=1}^r (x_{i+} \times x_{+i})}{N^2 - \sum_{i=1}^r (x_{i+} \times x_{+i})} \quad \text{Eq. (4)}$$

where r is the number of rows, x_{ii} is the number of observations in row i and column i , x_{i+} and x_{+i} are the marginal totals for row i and column i , respectively, and N is the total number of samples.

Calculation of Land Surface Metrics

Several landscape metrics were selected to characterize landscape features, including the number of patches, patch density, most extensive patch index, and total edge length (Table 2). These metrics were extracted from the land-use maps for each year using Fragstats software.

This study comprehensively analyzed land-use variety and changes to ensure accurate results. The first step involved using data on the number of patches (NP) for each land-use type in each year. Several numerical indices were calculated to assess the diversity of land-uses annually, including Margalef richness, Simpson's equitability, and the Shannon-Wiener diversity index. Margalef richness evaluates the number of distinct land-use types, providing insights into the overall variety. Simpson's equitability measures the evenness of distribution among land-use types, indicating uniformity. The Shannon-Wiener index combines the number and proportional distribution of land-use types, offering a comprehensive measure of diversity. Together, these indices enable a detailed understanding of land-use dynamics and changes over time, essential for informed land management and conservation strategies.

In the second step, parametric indices, including diversity grading curves, were used to analyze land-use diversity for each year graphically. The numerical indicators of land-use diversity were calculated annually, and the diversity rating curves were plotted using PAST software version 4.08.

A one-way analysis of variance (ANOVA) was conducted to examine differences in the studied metric indicators over time (1987 to 2022) across different land-use types. Tukey's test compared the average metrics between the various land-use types during the study periods. Both analyses

were performed using SPSS 24 software. To identify the most critical and sensitive variable metrics across land uses over time (1987 to 2022), a principal component analysis (PCA) was conducted in CANOCO 5.0 software.

Preparation of Nomadic Settlement Distribution Map

This research used Google Earth imagery and field observations to create a distribution map of nomadic settlements. This approach enabled precise identification and mapping of settlement locations. The high-resolution images provided by Google Earth facilitated the accurate detection of nomadic settlements across extensive areas. Field observations further validated the presence and exact locations of the settlements identified in the satellite images, ensuring the reliability and accuracy of the data.

Due to data availability constraints, distribution maps were specifically generated for 2010 and 2022. This temporal selection allowed for a comparative analysis of settlement patterns over 12 years, highlighting changes and trends in the distribution of nomadic populations.

Findings

The resulting maps provide valuable insights into the spatial dynamics of nomadic settlements. They can inform planning and policy decisions on land-use and resource management in the studied areas. This study offers a detailed analysis of land-use changes in the Arasbaran forests, focusing on four key land cover classes—forest, rangeland, agriculture,

Table 2) Landscape parameters used in the study (Fragstats Software Guide).

Metric name	Explanation	Range	Unit
Number of patches (NP)	The total number of patches for a particular class	NP ≥1	-
Largest patch index (LPI)	It shows the percentage of the landscape that consists of the biggest patch	100≤0<LPI	Percent
Patch density (PD)	It shows the number of patches in 100 hectares.	PD>0	Number of patches per 100 ha
Total edge of patch (TEP)	The total perimeter of patches of a class	TPE>0	meter

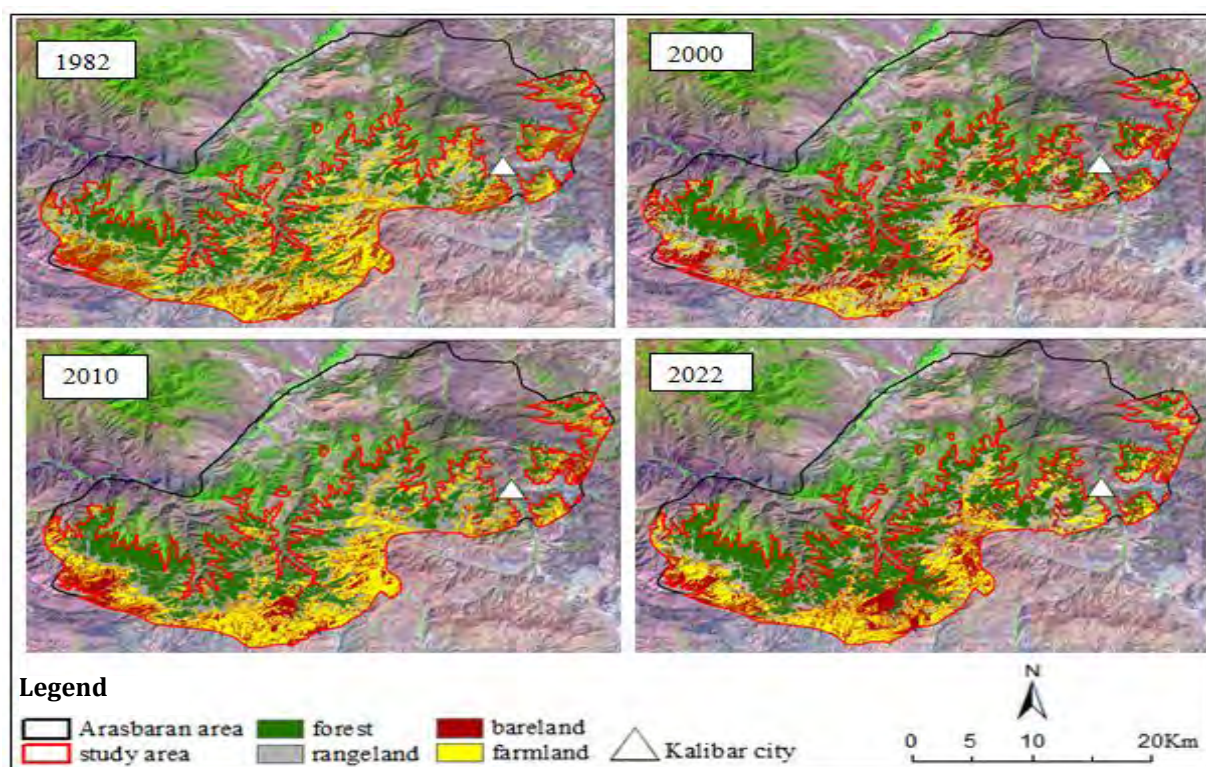


Figure 2) Land-use maps in 1987, 2000, 2010, and 2022.

and bareland—across four snapshots, including 1987, 2000, 2010, and 2022.

Table 3 presents the validation results of image classification for land-use across four years: 1987, 2000, 2010, and 2022. For the forest class, the User's Accuracy remains consistently high (91.67% to 100%) across all years, with Producer's Accuracy maintaining a perfect 100%. Rangeland showed variability, with User's Accuracy ranging from 77.78% to 94.12% and Producer's Accuracy between 82.35% and 88.89%. Agriculture exhibits more fluctuation, with User's Accuracy ranging from 63.64% to 87.5%, while Producer's Accuracy improves from 69.23% in 1987 to 86.67% in 2022. Bareland shows a slight decline in Producer's Accuracy, but User's Accuracy remains relatively stable, ranging from 84.21% to 94.44%. Overall classification accuracy remains above 85% in all years, with Kappa coefficients consistently above 0.80, indicating substantial agreement between the classified maps and ground truth data. Figure 2 displays the land-use maps for the four studied

classes—forest, rangeland, agriculture, and bareland—at altitudes above 1,500 meters in the Arasbaran forests across four years.

The region's total area at elevations above 1,500 meters is 96,865 hectares. Based on the land classification results across the four years studied, forest cover consistently occupied the most considerable portion of this area. Forested land reached its peak in 2000 and 2022 (Figure 3).

The number of changes in land use across the region, measured in hectares over three time periods, is summarized in Table 4. According to the results, forest and rangeland areas increased during the first period (1987-2000), decreased in the second period (2000-2010), and then increased again in the third period (2010-2022). Agricultural land area declined in the first period but increased in the second and third periods. Bareland decreased during the first and second periods but increased in the third. From 1987 to 2000, 20.22% of the region changed. The most significant change was in

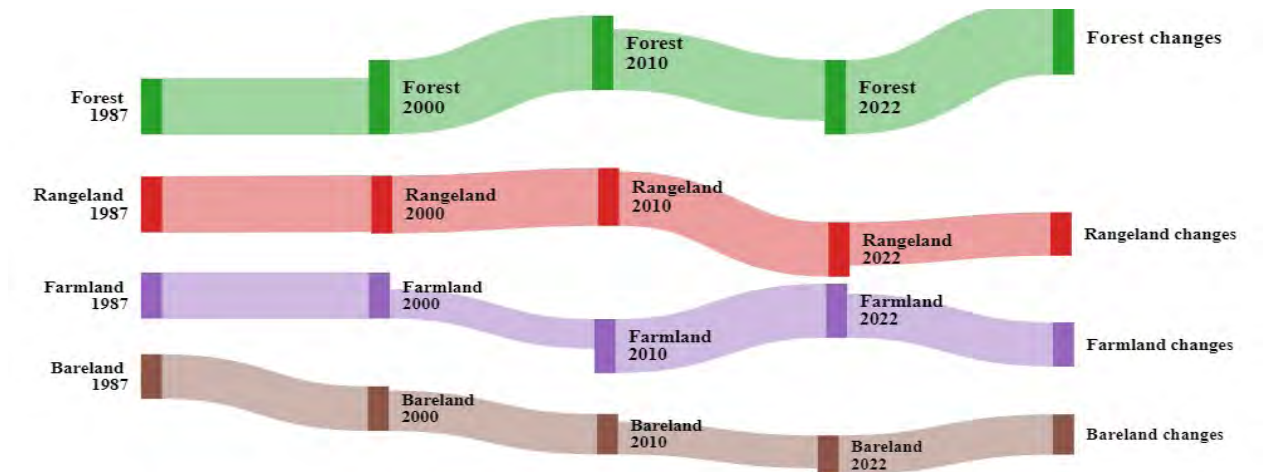


Figure 3) The area of the studied land-uses in the Arasbaran Region.

forest land, which expanded by approximately 8,907 hectares, mainly due to the conversion of 9,819 hectares from rangeland to forest. From 2000 to 2010, 24.12% of the region experienced changes, the most notable being an 11,667-hectare increase in agricultural land, primarily from the conversion of 8,195 hectares of rangeland. Finally, between 2010 and 2022, 20.7% of the area changed, with forest land showing the most significant increase-6,492 hectares-mainly due to the conversion of 6,646 hectares from rangeland to forest.

Measures of the Landscape of the Land

Figure 4 presents the patch count analysis results for four land cover types—forest, rangeland, agriculture, and bareland—in 1987, 2000, 2010, and 2022.

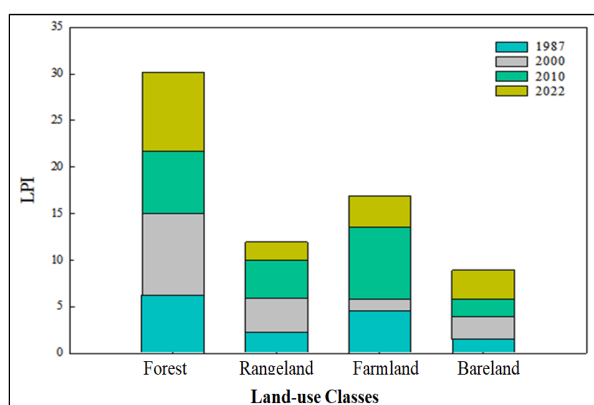


Figure 4) The results of calculating the number of patches (NP) in four land-use classes in 1987, 2000, 2010, and 2022.

Table 5 presents the results of patch density (PD) and total patch edge (TEP) measurements for five land-use types—forest, rangeland, agriculture, and bareland—over 1987, 2000, 2010, and 2022. Patch density (PD) indicates the number of patches per unit area, and total patch edge (TEP) represents the total boundary length of all patches within a land-use type. Forest land shows a decline in patch density from 1987 to 2000, followed by a gradual increase in 2022, while its total edge also decreases over time but starts to rise again by 2022. Rangeland shows a fluctuating trend in patch density and total edge, increasing in 2000 and 2022. Agriculture exhibits a decrease in patch density and total edge after 2000, while bareland shows an overall increase in patch density, with a rise in the total patch edge between 1987 and 2022. These results highlight the dynamic changes in land-use patterns over the 35 years.

Figure 5 illustrates the calculation of the Largest Patch Index (LPI) for four land-use classes—forest, rangeland, agriculture, and bareland—across the years 1987, 2000, 2010, and 2022. The LPI represents the percentage of the landscape occupied by the largest patch within each land-use type, providing insights into landscape dominance and fragmentation. Over the years, the forest

Table 3) The results of validation of image classification.

Land-use class/year	1987		2000		2010		2022	
	User's Accuracy	Producer's Accuracy	User's Accuracy	Producer's Accuracy	User's Accuracy	Producer's Accuracy	User's Accuracy	Producer's Accuracy
Forest	91.7	100	91.7	100	100	100	95.6	100
Rangeland	77.8	82.3	77.8	82.3	94.1	88.9	80	88.9
Agriculture	75	69.2	87.5	53.8	63.6	77.8	72.2	86.7
Bareland	94.4	85	90.9	100	84.2	72.7	88.9	72.7
Overall accuracy	86.1		87.5		85.5		86.2	
Kappa Coefficient	0.81		0.82		0.81		0.82	

Table 4) Type and number of changes made from 1987-2000.

Type of change/ year	1987-2000		2000-2010		2010-2022	
	ha	Percent	ha	Percent	ha	Percent
Forest	8907	9.20	-6473	-6.68	6492	6.70
Rangeland	879	0.91	-1579	-1.63	5298	5.47
Agriculture	-7785	-8.04	11667	12.04	-4714	-4.87
Bareland	-2001	-2.07	-3624	-3.75	3515	3.62
Forest no change	24807	25.61	28672.00	29.00	28343.7	31.26
Forest to rangeland	1747	1.80	6657.5	6.87	750	0.83
Forest to agriculture	45.7	0.05	102.7	0.11	13.4	0.01
Forest to bareland	122	0.13	197	0.20	49.4	0.05
Rangeland no change	13450	13.9	15657	16.16	14709	16.22
Rangeland to forest	9819	10.14	426	0.44	6646	7.33
Rangeland to agriculture	1713	1.77	8195	8.46	2476.5	2.73
Rangeland to bareland	1791.5	1.85	3374.6	3.49	2242.7	2.47
Agriculture no change	8258.5	8.53	10090	10.42	13588	14.98
Agriculture to forest	869	0.90	19	0.02	395	0.44
Agriculture to rangeland	7831	8.08	1573.7	1.62	3936	4.34
Agriculture to bareland	5048	5.21	2538.2	2.62	2536	2.79
Bareland, no change	12400	12.8	9627	9.95	9006	9.93
Bareland to forest	134	0.14	39	0.04	264	0.29
Bareland to rangeland	4625	4.77	2186	2.26	1380	1.52
Bareland to agriculture	4203	4.34	7500	7.74	5095	5.62

Table 5) The results of the calculation of patch density measurements and total patch edge in five land-uses during 1987-2022

Land-use	Patch Density (PD)				Total Edge of Patch (TEP)			
	1987	2000	2010	2022	1987	2000	2010	2022
Forest	5.5	3.0	3.1	3.8	5146350	3555630	3839670	4251270
Rangeland	9.7	11.6	8.6	12.9	10002510	9819000	8465910	8049330
Agriculture	13.3	13.6	9.9	9.9	9780480	6999180	9077280	7554870
Bareland	10.0	12.5	14.4	12.7	6930630	7202640	6821100	7774770

land-use shows a fluctuating trend in LPI, with significant increases in 2000 and 2022, indicating larger contiguous forest patches during these periods. Rangeland and agriculture show varied trends, with both land-use types experiencing shifts in dominance at different times. Bareland exhibits more stability, with moderate changes in LPI throughout the periods. These trends highlight the shifting landscape composition and the changing dominance of different land uses over time.

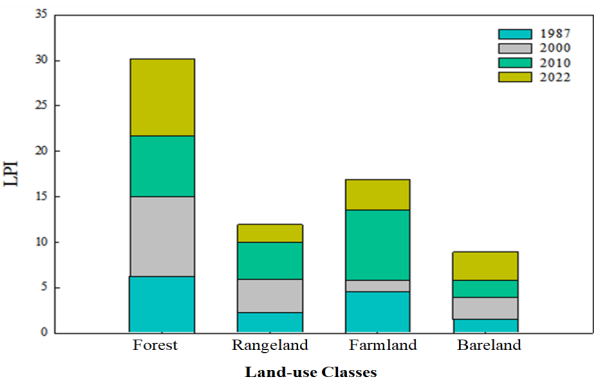


Figure 5) The results of calculating the largest patch index (LPI) in four land-use classes in 1987, 2000, 2010, and 2022.

Numerical Diversity Indices of the Land-Use Type in Different Years

Table 6 presents the indicators of equitability, richness, and diversity based on the Number of Patches (NP) index for different land-use types across the studied periods: 1987, 2000, 2010, and 2022. The Shannon index (Shannon_H) reflects the diversity of land-use, with values showing a slight decrease

from 1987 to 2010, followed by a modest increase in 2022. The Margalef richness index, which assesses the number of different land-use types, has remained relatively stable over the years, with the highest value recorded in 2010. The Equitability index (Equitability_J) indicates how evenly the land-use types are distributed, showing a decline from 1987 to 2000, followed by slight increases in subsequent years. These indicators suggest fluctuations in land-use diversity and distribution, emphasizing the dynamic nature of land cover changes over the examined periods.

Table 6) The indicators of equitability, richness, and diversity in the studied periods based on the NP index related to land-use type.

Time series	Shannon_H	Margalef	Equitability_J
Np1987	1.342	0.285	0.968
NP2000	1.280	0.283	0.923
NP2010	1.275	0.287	0.920
NP2022	1.304	0.284	0.940

The diversity profile for 1987 stands out as distinct, remaining uninterrupted by the profiles of subsequent years and positioned higher than those of later years. This indicates that land-use diversity was more significant in 1987 than in other years (Figure 6). Following 1987, the profile for 2022 ranks second, remaining separate from any other profiles, suggesting a decrease in diversity since 1987, placing it in a lower category.

Table 7) Variance analysis of changes between different land uses from 1987-2022.

	Source of Variation	df	Sum of Squares	Mean Square	F	P-Value
NP	Between groups	3	170131123.5	56710374.50	20.14	**0.00
	Within groups	12	33779932.50	2814994.37		
	Total	15	203911056			
LPI	Between groups	3	66.10	22.03	8.56	**0.00
	Within groups	12	30.88	2.57		
	Total	15	96.98			
PD	Between groups	3	185.54	61.84	20.15	**0.00
	Within groups	12	36.83	3.06		
	Total	15	222.37			
TE	Between groups	3	5.55	1.85	22.54	**0.00
	Within groups	12	9.85	8.21		
	Total	15	6.54			

** Significant differences at the level of 1%

In contrast, the profiles for 2000 and 2010 intersect, making it challenging to compare these two periods in terms of their numerical indicators and overall land-use diversity. In summary, 1987 ranks highest in user diversity, followed by 2022 in second place, while 2000 and 2010 are tied for third.

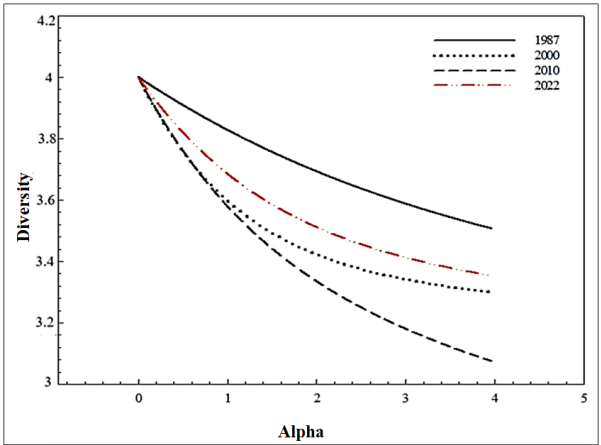


Figure 6) Diversity profiles of four years using Renyi's diversity ($H\alpha$). The scale parameter (α) gives the order of Renyi's diversity; $\alpha = 0$ is the logarithm of species richness, $\alpha = 1$ equals the Shannon diversity index, $\alpha = 2$ is the logarithm of the reciprocal equability index, $\alpha = \text{Inf}$ refers to the proportion of the most abundant species.

Table 7 presents the results of a variance

analysis examining changes in land-use between 1987 and 2022, focusing on four key indicators: Number of Patches (NP), Largest Patch Index (LPI), Patch Density (PD), and Total Edge (TE). The results reveal significant differences between the groups for all indicators, indicating a high level of statistical significance (at the 1% level). Specifically, NP, LPI, PD, and TE showed substantial variations in land-use characteristics over the studied period. The significant results imply that changes in land-use patterns from 1987 to 2022 are noteworthy, highlighting the need for further investigation into the factors contributing to these shifts.

The results of the PCA analysis, aimed at identifying the most significant and sensitive variable parameters among land uses over time, are illustrated in Figure 7. This figure reveals that the Largest Patch Index (LPI) vector tends to align closely with forest use in most years, particularly in 2022, indicating that forest use has the highest LPI. The first axis clearly distinguishes forest use from the other three categories, as shown in the Table and Figure 7. The parameters associated with

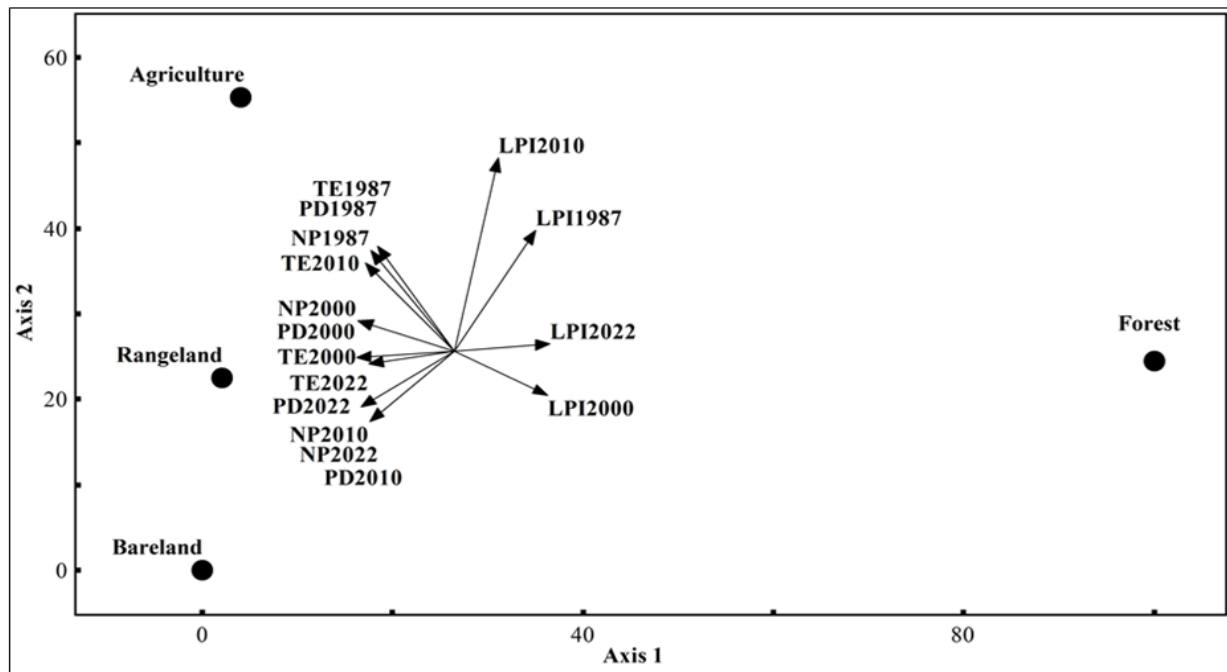


Figure 7) PCA analysis between land-uses over time.

an eigenvector greater than 0.9 on this axis play a crucial role in differentiating these land-uses, highlighting them as the most sensitive parameters. Specifically, LPI values for 2022 and 2000 emerge as key indicators for the transition to forest use, reflecting an increase in these values within forested areas. Conversely, the number of patches (NP) and patch density (PD) indices for 2000, along with NP, PD, and total edge (TE) indices for 2022, show a decline in forest use, while these indices increase in the other three land-uses, particularly rangelands.

On the second axis, only the LPI for 2010 stands out as a significant indicator (with an eigenvector greater than 0.9) that separates bareland from agricultural land. However, it does not distinguish between other uses. Generally, this index increases with the transition to agricultural use and decreases with the conversion to bareland. Additionally, the results in Figure 5 confirm that the LPI value for agricultural use in 2010 significantly differed from that of bareland, with agricultural use exhibiting the highest LPI during this period.

Discussion

The extent of forest land cover is now a vital indicator of development, underscoring the importance of effectively managing forest resources to enhance their quantity and quality. The results indicate a substantial increase in forest cover, rising by 21.9% in 2022 compared to 1987. In contrast, rangeland decreased by 6.19%, agricultural land-use fell by 0.86%, and bareland decreased by 2.16% during the same period. This trend suggests that while forest cover has expanded, agricultural land, rangelands, and bareland have diminished in the studied area, likely due to protective management measures, law enforcement, and improved facilities for local communities surrounding the forests. Sasanifar et al. (2019) concluded that longstanding conservation laws in the Arasbaran forests have positively influenced forest characteristics. This finding is further supported by ^[35] and ^[36], highlighting the benefits of forest protection measures. Although the forest area in 1987 was smaller compared to 2022, the number of forest patches was higher in 1987. This suggests

that the increase in forest area by 2022 has resulted in the connectivity of forest patches, reducing the overall number of patches. Such continuity may have enhanced the chances of survival of animal species like the BG, potentially expanding the habitat range of this endangered species. Gottschalk et al. (2007) examined the distribution of the BG in the Caucasus and Turkey, noting that reducing forest patches—due to factors like easier access for hunting and habitat limitation—can contribute to a decline in bird populations. Furthermore, the observed decrease in agricultural land-use, coupled with an increase in rangeland and barren land patches, suggests fragmentation within these ecosystems. In areas designated for agricultural use, such as Bata, the number of patches associated with agricultural land has increased despite reducing the total agricultural area by 2022. This indicates that agriculture thrives in small plots within these forested regions. The dispersion and intermingling of various land uses in the high-altitude habitats of the BG species highlight the need for more detailed studies to understand the specific effects of land-use changes on this species.

The analysis of the spot density index revealed a decrease in this metric for forest land-use in 2022 compared to 1987. Specifically, the average number of forest patches per 100 hectares in 2022 was 3.82, down from 5.48 in 2016. This decline suggests an expansion of forest cover and increased patch connectivity resulting from the reduced patch density index. Such connectivity may create favorable conditions for the growth of the grouse population. Baskaya (2003) identified habitat destruction, forest fragmentation, and concentrated forestry practices as critical threats to this species' habitat in the mountainous regions of Turkey. Sefidi and Ghanbari ^[37] conducted a quantitative study

on tree saplings in the BG habitat within Arasbaran. They concluded that forest areas with a higher density of suitable conditions and dense stands provide optimal habitats for this bird. These ideal conditions arise from intact forests characterized by high continuity and minimal human interference. Conversely, the results for the spot density index regarding agricultural use indicate a decrease in 2022, while the index for rangeland land-use shows an increase. This suggests that the reduction in agricultural land-use has resulted in the disappearance of some agricultural patches, which have subsequently transformed into barren lands or rangelands. Consequently, this trend has led to an increase in the number of patches for both bareland and rangeland in 2022. The total edge of the patch index indicates a decrease in the boundary of forest land-use in 2022, reflecting the connectivity of existing patches and a reduction in the overall edge. This reduction suggests a decrease in external pressures on the forest environment, thereby creating more favorable conditions for the presence of the BG species. Faridi and Naseri (2019) noted that this species thrives in dense and semi-dense forests in Arasbaran. Thus, by enhancing the connectivity of forest patches and minimizing their exposure to external threats, factors such as hunting, human entry, and livestock grazing can be effectively mitigated ^[38]. Behruzi Rad (2016) identified the destruction of forest habitats and livestock grazing as the primary threats to the BG species in the region. Furthermore, the observed decrease in the boundary between rangeland and agricultural land, coupled with an increase in bareland, suggests that future protective measures could significantly reduce the impact of agriculture and grazing in the area ^[39].

The investigation into the most extensive patch index revealed that forest land-use in 2022 accounted for 8.5% of the total

area, a significant decline from 24.9% in 1987. Additionally, the LPI index for both rangeland and agricultural land uses has decreased over the past 35 years, while it has increased for barren lands. Expanding forest cover creates more significant challenges for accessing deeper forest areas. It contributes to the stability of the ecosystem, which benefits various animal and plant species, including the grouse. Previous studies have indicated that a reduction in the size of forest land-use patches typically reflects increased human interference and intervention ^[40].

Overall, the results suggest that 2000 and 2010 exhibited similar land-use diversity, indicating minimal changes and relative stability in land-use patterns. Furthermore, the latest data from 2022 demonstrate a significant trend toward connecting forest patches and enhancing their continuity. These developments are expected to foster improved protection and growth of forest areas, ultimately increasing plant and animal biodiversity.

The results of this study provide critical insights into the ecological needs of the Caucasian Black Grouse (BG) by establishing a link between land-use changes and the species' habitat requirements, particularly for nesting and foraging. The observed fluctuations in forest and rangeland cover, patch density, and the Largest Patch Index (LPI) reflect the dynamic landscape of the Arasbaran forests, which are vital for BG's survival. Periods of forest expansion, particularly noted in 2000 and 2022, suggest an increase in BG's potential nesting and foraging grounds, as these areas offer essential shelter and food resources (20, 38). Conversely, reducing forest cover and increasing agricultural land in other periods may lead to habitat fragmentation, creating challenges for BG by reducing continuous habitat patches and increasing edge effects, which can adversely impact

nesting sites under bushes and rocks ^[41, 42]. Understanding these patterns is crucial for planning effective conservation strategies to maintain and restore forest and rangeland areas to support BG's ecological needs, ensuring the species' survival and enhancing habitat quality. Previous studies have also emphasized the importance of habitat modeling and spatial analysis in assessing and mitigating threats to BG populations ^[10, 14]. Therefore, integrating these findings with spatial modeling tools can enhance conservation efforts, as demonstrated by applying geographical information systems (GIS) and maximum entropy methods in predicting BG habitat suitability ^[38]. The literature consistently highlights the necessity of preserving contiguous forest landscapes to mitigate habitat fragmentation and its adverse impacts on BG populations ^[11]. Overall, this study reinforces the importance of adaptive land management practices that align with the ecological needs of the BG, supporting their habitat preferences and contributing to the broader conservation objectives in the Arasbaran biosphere reserve.

Conclusion

This study emphasizes the critical role of forest land cover as an indicator of development, highlighting the need to manage forest resources to improve their quantity and quality effectively. The results reveal a significant increase in forest cover of 21.9% by 2022 compared to 1987, alongside declines in rangeland (6.19%), agricultural land (0.86%), and bareland (2.16%). These changes indicate that enhanced protective management, law enforcement, and improved facilities for local communities have facilitated forest expansion and reduced other land uses. The findings align with previous studies that underscore the positive impact of conservation laws on

forest characteristics. Interestingly, while the forest area was smaller in 1987, the number of forest patches was more remarkable, suggesting that the increase in forest area by 2022 has led to improved interconnection and reduced fragmentation of forest patches. This continuity is likely beneficial for species such as the black grouse, whose habitats are adversely affected by fragmentation. Conversely, fragmentation of agricultural and barren lands has increased, indicating that agricultural practices persist in smaller plots within forested areas.

The analysis of the spot density index indicates a decrease in this index for forest land-use in 2022, reflecting more extensive and continuous forest patches. This continuity creates better conditions for species growth, particularly the BG, which thrives in dense, uninterrupted forests. The reduction in the border of forest land-use further illustrates the diminishing external impacts on forest environments, enhancing habitat quality for various species. Overall, the findings suggest a positive trend toward greater continuity of forest cover and reduced land-use fragmentation, contributing to improved ecosystem stability and biodiversity. The results highlight the importance of sustained protective measures to preserve and enhance forest ecosystems, ultimately supporting the conservation of plant and animal species in the region.

Acknowledgments

We sincerely appreciate from University of Tabriz for financial support.

Ethical Permission: All works have been approved by the University of Tabriz.

Authors Contribution: Conceptualization, S.G., S.S., and P.Á.-Á.; Methodology, S.G., S.S. and P.Á.-Á.; Software, S.G., Z.N., and P.Á.-Á.; Formal analysis, S.G., Z.N., and S.S.; Investigation, S.G.; Resources, S.G.; Data curation, S.G.; Writing-original draft preparation, S.G., P.Á.-Á., S.S., and

P.Á.-Á.; Writing-review and editing, P.Á.-Á.; Funding acquisition, S.G. All authors have read and agreed to the published version of the manuscript.

Conflicts of Interest: There is no conflict of interest.

Funding/Supports Sections: This work is supported by the University of Tabriz.

References

1. Jantz S.M., Barker B., Brooks T.M., Chini L.P., Huang Q., Moore R.M., Noel J., Hurtt G.C. Future habitat loss and extinctions driven by land-use change in biodiversity hotspots under four scenarios of climate-change mitigation. *Conserv. Biol.* 2015; 29(4):1122-1131.
2. Ghanbari S., Sefidi K. Characteristics of *Viburnum lantana* L., Stands in the Lowest Limit of Its Distribution in the Arasbaran Forests, Iran. *ECOPERSIA* 2023; 11(1):25-36.
3. Xu L., Chen S.S., Xu Y., Li G., Su W. Impacts of land-use change on habitat quality during 1985–2015 in the Taihu Lake Basin. *Sustainability*. 2019; 11(13):3513.
4. Allan J.R., Watson J.E., Di Marco M., O'Bryan C.J., Possingham H.P., Atkinson S.C., Venter O. Hotspots of human impact on threatened terrestrial vertebrates. *PLoS Biol.* 2019; 17(3):e3000158.
5. Ndegwa Mundia C., Murayama Y. Analysis of land-use/cover changes and animal population dynamics in a wildlife sanctuary in East Africa. *Remote Sens.* 2009; 1(4):952-970.
6. Clark N.E., Boakes E.H., McGowan P.J., Mace G.M., Fuller R.A. Protected areas in South Asia have not prevented habitat loss: a study using historical models of land-use change. *PloS One*. 2013; 8(5):e65298.
7. Rahdari V., Maleki Najafabadi S., Afsari K., Abtin A., Piri H., Fakhire A. Monitoring the changes in land-use and land cover of Hamon Wildlife Sanctuary during the 1986 to 2009 using satellite images and geographic information systems. *Iran. Remote Sens. GIS*. 2011; 3(2):59-70.
8. Najafi Z., Darvishsefat A., Fatehi P., Attarod P. Time series analysis of vegetation dynamic trend using Landsat data in Tehran Megacity. *Iran. J. Forest*. 2020; 12(2):257-270.
9. Foroutan S., Islamzadeh N. The Study of Mazandaran Province Forest and Rangeland Vegetation Changes Trend by Satellite Images. *Plant Ecosys. Conserv.* 2022; 9(19):197-215.
10. Baskaya S. Distribution and principal threats to Caucasian black grouse *Tetrao mlokosiewiczii* in the Eastern Karadeniz Mountains in Turkey.

- Wildlife Biol. 2003; 9(4):377-383.
11. Storch I. Conservation status of grouse worldwide: an update. Wildlife Biol. 2007; 13(sp1):5-12.
 12. Darvishi A., Fakheran S., Soffianian A., Ghorbani M. Quantifying landscape spatial pattern changes in the Caucasian Black Grouse (*Tetrao Mlokosiewiczii*) Habitat in Arasbaran biosphere reserve. Iran. J. Appl. Ecol. 2014; 2(5):27-38.
 13. Kaboodvandpour S., Shiriazar J. Modeling the habitat desirability of the Black Grouse species (*Tetrao mlokosiewiczii*) in Arasbaran biosphere reserve by maximum entropy method. International Congress of Developing Agriculture, Natural Resources, Environment and Tourism of Iran. 2019:14-6.
 14. Darvishi A., Fakheran S., Soffianian A. Monitoring landscape changes in Caucasian black grouse (*Tetrao mlokosiewiczii*) habitat in Iran during the last two decades. Environ. Monit. Assess. 2015; 187(7):443.
 15. Etzold J. Analyses of vegetation and human impacts in the habitat of the Caucasian Black Grouse *Tetrao mlokosiewiczii* in the Greater Caucasus/Azerbaijan. Archiv für Naturschutz und Landschaftsforschung. 2005; 44:7-36.
 16. Ghanbari S., Nasiri V., Mohammadi Y. Effects of developmental level on forest area changes of rural areas in Arasbaran by satellite images. Plant Ecosyst. Conserv. 2019;7(14):291-312.
 17. Ghanbari S., Turvey S.T. Local ecological knowledge provides novel evidence on threats and declines for the Caucasian grouse *Lyrurus mlokosiewiczii* in Arasbaran Biosphere Reserve, Iran. People Nat. 2022; 4(6):1536-1546.
 18. Sagheb-Talebi K., Pourhashemi M., Sajedi T. Forests of Iran: A Treasure from the Past, a Hope for the Future: Springer. 2014: 152 pp.
 19. Sasanifar S., Alijanpour A., Shafiei A.B., Rad J.E., Molaei M., Azadi H. Forest protection policy: Lesson learned from Arasbaran biosphere reserve in Northwest Iran. Land Use Policy. 2019; 87:104057.
 20. Ghanbari S., Sefidi K., Álvarez-Álvarez P. Vegetation and Forest Complexity Analysis of the Caucasian Grouse (*Lyrurus mlokosiewiczii*) Habitats in the Lesser Caucasus Mountain. Forests. 2023; 14(2):353.
 21. Ghanbari S., Sasanifar S. Agroforestry Systems in Arasbaran Region, Obstacles and Opportunities for Farmers in Combating with Climate Change. ECOPERSIA 2024; 12(4):363-77.
 22. Rouse J.W., Haas R.H., Schell J.A., Deering D.W. Monitoring vegetation systems in the Great Plains with ERTS. NASA Spec Publ. 1974; 351(1):309.
 23. Qi J., Chehbouni A., Huete A.R., Kerr Y.H., Sorooshian S. A modified soil adjusted vegetation index. Remote Sens. Environ. 1994; 48(2):119-126.
 24. Huete A., Liu H., Batchily K., Van Leeuwen W. A comparison of vegetation indices over a global set of TM images for EOS-MODIS. Remote Sens. Environ. 1997; 59(3):440-451.
 25. Muchsin F., Dirghayu D., Prasasti I., Rahayu M., Fibriawati L., Pradono K., Mahatmanto B. Comparison of atmospheric correction models: FLAASH and 6S code and their impact on vegetation indices (case study: paddy field in Subang District, West Java). IOP Conference Series: Earth and Environmental Science; 2019: IOP Publishing.
 26. Cooley T., Anderson G.P., Felde G.W., Hoke M.L., Ratkowski A.J., Chetwynd J.H., Gardner J.A., Adler-Golden S.M., Matthew M.W., Berk A. FLAASH, a MODTRAN4-based atmospheric correction algorithm, its application and validation. IEEE international geoscience and remote sensing symposium; IEEE. 2002;3(1):1418-1414.
 27. Berk A., Anderson G.P., Bernstein L.S., Acharya P.K., Dothe H., Matthew M.W., Adler-Golden S.M., Chetwynd Jr J.H., Richtsmeier S.C., Pukall B. MODTRAN4 radiative transfer modeling for atmospheric correction. Optical spectroscopic techniques and instrumentation for atmospheric and space research III; SPIE. 1999; 3756(1): 348-353.
 28. Yang M., Hu Y., Tian H., Khan F.A., Liu Q., Goes J.I., Gomes H.D.R., Kim W. Atmospheric correction of airborne hyperspectral CASI data using polymer, 6S, and FLAASH. Remote Sens. 2021; 13(24):5062.
 29. Wang Z., Xia J., Wang L., Mao Z., Zeng Q., Tian L., Shi L. Atmospheric correction methods for GF-1 WFV1 data in hazy weather. J. Indian Soc. Remote Sens. 2018; 46(1): 355-366.
 30. Shalaby A., Tateishi R. Remote sensing and GIS for mapping and monitoring land cover and land-use changes in the Northwestern coastal zone of Egypt. Appl. Geogr. 2007; 27(1):28-41.
 31. Günlü A., Sivrikaya F., Baskent E.Z., Keles S., Çakir G., Kadiogullari A.İ. Estimation of stand type parameters and land cover using Landsat-7 ETM image: A case study from Turkey. Sensors. 2008; 8(4):2509-2525.
 32. Serra P., Pons X., Saurí D. Land-cover and land-use change in a Mediterranean landscape: a spatial analysis of driving forces integrating biophysical and human factors. Appl. Geogr. 2008; 28(3):189-209.
 33. Heidarlou H.B., Mirshekarlou A.K., Lopez-Carr D., Borz S.A. Conservation policy and forest transition in Zagros forests: Statistical analysis of human welfare, biophysical, and climate drivers. For. Policy Econ. 2024; 161:103177.
 34. Rash A., Mustafa Y., Hamad R. Quantitative assessment of Land-use/land cover changes

- in a developing region using machine learning algorithms: A case study in the Kurdistan Region, Iraq. *Heliyon*. 2023; 9(11):1-20..
35. Ribeiro M.P., de Mello K., Valente R.A. How can forest fragments support protected areas connectivity in an urban landscape in Brazil? *Urban For. Urban Gree*. 2022; 74:127683.
 36. Negassa M.D., Mallie D.T., Gameda D.O. Forest cover change detection using Geographic Information Systems and remote sensing techniques: a spatio-temporal study on Komto Protected forest priority area, East Wollega Zone, Ethiopia. *Environ. Syst. Res*. 2020; 9(1):1-14.
 37. Sefidi K., Ghanbari S. Quantitative analysis of woody plants within the habitat of Caucasian black grouse (*Lyrurus mlokosiewiczii* Taczanowski) in the Arasbaran Forests, Iran. *Iran. J. Forest Poplar Res*. 2021; 29(3):301-313.
 38. Faridi E., Naseri D. Providing a habitat model for black male Caucasians grouse (*Tetrao mlokosiewiczii*) using geographical information system (GIS). *J. Environ. Sci. Technol*. 2019; 21(5):263-272.
 39. Behruzi Rad B. Biology of Caucasian black grouse. 3rd National Conference on Biology and Natural Science of Iran. 2016:8.
 40. Karami A., Fegghi J. Investigation of Quantitative metrics to protect the landscape in land-use by sustainable pattern (Case study: Kohgiluyeh and Boyer Ahmad). *J. Environment. Studie*. 2012; 37(60):79-88.
 41. Gottschalk T.K., Ekschmitt K., İsfendiyaroglu S., Gem E., Wolters V. Assessing the potential distribution of the Caucasian black grouse *Tetrao mlokosiewiczii* in Turkey through spatial modelling. *J. Ornithol*. 2007; 148(4):427-434.
 42. Yousefi M., Darvishi A., Tello E., Barghjelveh S., Dinan N.M., Marull J. Comparison of two biophysical indicators under different landscape complexity. *Ecol. Indic*. 2021; 124:107439.